



Manuscript ID ZUMJ-2212-2705 (R3)

Manuscript ID ZUMJ-2212-2705 (R3)

## ORIGINAL ARTICLE

# Immunohistochemical Expression of Aquaporin 8 in the Sublingual Salivary gland of High Fat Diet /Fructose Rat Model

Amal. S. Hamada\*, M. Hendawy, Sherif RN, Adel A. Elhawary.

Anatomy and Embryology Department, Faculty of Medicine, Mansoura University, Mansoura, Egypt

### \*Corresponding author:

Anatomy and Embryology  
Department, Faculty of  
Medicine, Mansoura University,  
Mansoura, Egypt

E-mail: [amlsaber@mans.edu.eg](mailto:amlsaber@mans.edu.eg)

Submit Date 2022-12-28

Revise Date 2023-01-26

Accept Date 2023-02-03

### ABSTRACT

**Background:** Obesity affects multiple organs in the body including salivary glands resulting in secretory dysfunction. The selective water channels, aquaporins (AQPs) have a role in salivary secretion. As far as the authors know, no previous research has been done to investigate the effect of a high fat diet on AQ8 localization in sublingual glands (SLGs).

**Methods:** 12 male Sprague-Dawley albino rats were equally divided into two groups: a control group and a high fat diet (HFD) group. After 12 weeks, their blood glucose, insulin, serum triglyceride, cholesterol, HDL and LDL were evaluated. SLGs were dissected out and stained by H&E, PAS/Alcian and immunohistochemically using anti-smooth muscle actin ( $\alpha$  SMA) and anti- AQ8 antibodies. **Results:** Compared to the control group, blood insulin resistance, serum triglyceride, cholesterol, LDL levels were highly significantly increased, while HDL was highly significantly decreased. HFD SLGs were distorted with vacuolations, thick fibrous septa and congested blood vessels. Diameters were decreased. Image analysis of PAS/Alcian and  $\alpha$  SMA showed a highly significant increase in the (alcian blue) and a significant increase in the area % of  $\alpha$  SMA, while the expression of AQ8 was highly significant decreased compared to the control group.

**Conclusions:** The decreased AQ8 immunoexpression in HFD rats might contribute to gland 'secretory dysfunction.

**Key words:** high fat diet, Alcian blue,  $\alpha$  SMA, AQ8 immunohistochemistry, sublingual gland.



### INTRODUCTION

Obesity has become a pandemic in recent years, with an increasing prevalence especially amongst children and young people (1). A primary cause of obesity is overindulgent food intake; especially of carbohydrates that have been heavily processed (2). The rising numbers of people suffering from obesity poses a major public health threat, as it is associated with many diseases as comorbidities such as higher cardiovascular diseases risk as well as type 2 Diabetes Mellitus and some forms of cancer (3).

Although several factors have been implicated in causing obesity, the alarming rate of its increasing incidence suggests a greater role for behavioral and environmental factors (including diet) rather than genetic factors (4). Because of this, when studying models that study obesity caused by diet, polygenetic animals are preferred to monogenetic models (5).

Obesity has deleterious effects on multiple organs. When it comes to oral health, the association of obesity with xerostomia, periodontal disease and tooth decay has been discussed, in particular

attentions have been drawn to the microflora of the oral cavity due to obesity. In the salivary glands, changes to the morphology and function have been reported with obesity (6).

Aquaporins (AQPs) are integral membrane proteins that form channels and are ubiquitously present in living organisms from bacteria to human (7). They enable the transport of water by osmosis across cell membranes and therefore control the transcellular movement of fluids. The primary purpose of salivary glands is to produce and secrete saliva, with aquaporins safeguarding water flow, and thus playing a vital role (8).

Thirteen AQPs have been identified in human beings named (AQP 0 to AQP 12). They are categorized into 3 groups: orthodox AQPs (which includes AQP0-2, 4-6 and AQP8), Aquaglyceroporins (which includes AQP3, 7, 9 and 10) and supra AQPs, which are also known as unorthodox AQPs (including AQP 11 and 12) (9). Aquaporin-8 (AQP8) can transport water, urea and ammonia. It is also a peroxiporin, and hence it plays an essential role in controlling hydrogen peroxide elimination (10).

AQP8 was reported to be localized in acinar cells of rat submandibular glands, particularly their basolateral membranes, thus postulating a possibility of their collaboration with AQP5, to provide a transcellular passageway for water from the interstitial fluid to the lumen of acinar cells during the formation of saliva (11, 12).

The expression of AQP 8 in the submandibular gland of high fat and diabetic rat model has been studied. As the nature of secretion of the two glands is different, other salivary glands might have a different localization of AQP8. Therefore, this study aims to establish the localization of AQP8 protein in sublingual gland (SLG) and to evaluate the consequence of high fat diet/fructose on its expression (13).

## METHODS

**Animals used:** Twelve pathogen-free adult male Sprague-Dawley albino rats weighing between 250-300 grams were purchased from Medical Experimental Research Center of Mansoura University (MERC) for experimental researches, Mansoura. Every three rats were housed in a cage and were maintained under stable conditions: temperature ( $21 \pm 2$  °C), humidity ( $60 \pm 5\%$ ), and a reversed light/dark (12/12 h) cycle, with access to water and food *ad libitum* for two weeks before the

experiment for acclimatization and to ensure normal growth and behavior. This work was carried out in Mansoura experimental research center (MERC).

### **High fat and fructose diet (HFFD) model:**

High fat diet consists of 45% fat (40% animal fat + 5% in basal diet) (14) and fructose 20% (20 g of fructose was diluted in 100mL of tap water) (15).

**Experimental design:** The rats were randomly separated into two groups (with 6 rats in each group); a control group, which fed on basal diet and water *ad libitum* for 12 weeks and a high fat and fructose diet (HFD) group, which fed on high fat diet and fructose and water *ad libitum* for 12 weeks.

**[I] Biochemical study:** At the assigned time, the rats were weighed and tail vein blood samples were drawn for the assessment of their levels of blood glucose, serum cholesterol, triglycerides, LDL as well as HDL. Then the rats were decapitated under halothane anesthesia.

### **1-Assessment of the levels of fasting blood glucose and insulin:**

The Fasting blood glucose of rats was measured in each group at the beginning of the experiment and before their sacrifice. Blood samples were obtained after 8 hours fasting and the glucose level was measured by glucometer (Accu-check glucometer, Byer, Germany). The level of insulin was evaluated by ELISA (Bio Vender, Brno, Czech). Insulin sensitivity was then calculated using the HOMA index of insulin resistance formula (HOMA-IR); that is,  $HOMA = (\text{fasting blood glucose (in mg/dl)} \times \text{fasting insulin level (in } \mu\text{IU/ml)}) / 405$  (16).

**2) Assessment of serum lipid profile:** Blood samples were collected after overnight fasting (12-14h) before the rats' sacrifice. The commercially available kits were utilized to measure the serum levels of total cholesterol (using MG, cat. No. MG230001), triglycerides (using MG, cat. No. MG314001) and HDL (using MG, cat. No. MG266001) using their respective assay endpoint kits. Moreover, the level of LDL cholesterol was estimated by utilizing the formula:  $LDL \text{ cholesterol} = \text{Total cholesterol} - \text{HDL cholesterol} - (\text{Triglycerides}/5)$ . (17).

**[II] Histological study:** After the rats' sacrifice, the sublingual glands were dissected out and processed for histological and immunohistochemical studies.

### **1) Hematoxylin & Eosin (H&E) stain and combined Periodic acid Schiff/Alcian blue stain:**

These tissues were fixed in modified Davidson's

fluid (30% of a 37-40% solution of formaldehyde, 5% glacial acetic acid, 15% ethanol and 50% distilled H<sub>2</sub>O) for 48 hours, they were placed in increasing grades of alcohol for dehydration, cleared in xylene and embedded in paraffin. Then, sections of tissues were cut and stained by using histological stains; hematoxylin & eosin stain to evaluate the structural changes of the gland with differentiation of neutral mucins from acid mucins.

**2) Alpha smooth muscle actin and aquaporin 8 immunohistochemical stains:** The immunohistochemical stain for Alpha smooth muscle actin was performed to evaluate its expression in the myoepithelial cells that surround the acini and the ducts. Immunohistochemical stain for anti-aquaporin 8 antibodies was used to examine the changes in the expression of AQ8 among the two groups. The tissue sections were mounted on glass slides coated with 50.1% poly-lysine. After deparaffination and rehydration, the endogenous biotin was blocked by biotin blocking system. The sections were de-waxed first, and then they were incubated in a 3% hydrogen peroxide solution in order to inhibit endogenous peroxidase activity. Then, they were washed in phosphate-buffered saline (PBS;0,1M) and incubated with normal goat serum (DAKO, Ely UK, 1:5 dilution of PBS). This was done to prevent primary antibody non-specific binding. These sections were incubated with primary antibodies (mouse monoclonal Anti-Actin, alpha smooth muscle) (DAKO clone 1A4, Ely UK, 1:50 dilution) and anti-AQP8 (rabbit polyclonal, 1:200, Genetex, California, USA). Overnight incubation at 4°C was performed with biotinylated goat anti-rabbit polyclonal (DAKO, Ely UK, 1:400 dilution). Lastly, streptavidin-biotin horse-radish peroxidase complex (DAKO, Ely UK) was used on the sections.

### **[III] Morphometric measurements:**

**1) Assessment of body and gland weight:** The rats' body weight was measured at the beginning of the experiment and before their sacrifice. Body mass index was calculated (body weight (gm)/square length(cm<sup>2</sup>). The rat's length was measured from the nose to the tail base (18). Weights of salivary glands were measured.

**2) Diameter of intra lobular ducts:** Diameter of 50 intra lobular ducts and 50 acini of sublingual glands were measured in the H&E slides between the two groups (control and high fat diet). The largest and the smallest diameter in each duct and acini were

measured then the average diameter was calculated as (largest diameter +smallest diameter/2) (19).

**3) Area percentage and the optical density:** Four non-overlapping random fields of two sections for each sublingual gland in each rat of the two groups were chosen and were photographed using the Olympus® SC100 digital camera coupled to a photomicroscope (Germany). The morphometric assessment was performed using NIH Image J program (National Institutes of Health, Bethesda, MD, USA), in accordance to the program instructions (20).

**4) Area fraction (%) of alpha smooth muscle actin and aquaporin 8:** The positive expression of aquaporin 8 and alpha smooth muscle actin was measured as the percentage of the area occupied by brown pixels (420 x 360 micron) in the examined fields (x400). Color deconvolution was applied from the plugin list, followed by choosing "H DAB". This resulted in the formation of three new images. Hematoxylin image was Color 1, the DAB image was Color 2 and the Color 3 was the image containing shades of both DAB and hematoxylin, the complementary image. Quantification was done using the DAB image. The list for Analyze was chosen then area fraction was selected from set measurements. (12,19, 21).

**5) Mean optical density (MOD) of Alcian blue, alpha smooth muscle actin and aquaporin 8:** Images were captured with 400× objective lens. The de-convoluted DAB image was assigned a histogram profile for analysis; H-DAB-vector was utilized in order to get 3 images whose colors differed: brown, green and blue. The DAB images calibration using the brown color was done by measuring the stained areas' mean intensity. **In alcian blue**, analysis was run by de-convoluted alcian blue &H. Alcian blue &H vector was used to get three distinctly colored images: dark blue, blue and orange. Dark blue color calibration of the Alcian blue & H images was done. To ensure appropriate comparisons, standardization of thickness of sections was considered. In order to avoid bias in the outcomes, empty areas were excluded from the measurements. For quantitative comparisons, conversion of intensity measurements was converted to optical Density (OD) by using the formula: **OD = log (maximum intensity / mean intensity)**, where the maximum intensity = 250; and mean intensity = mean gray value. (22).

## STATISTICAL ANALYSIS

The SPSS (Statistical package for social science) computer program version 26 was utilized for coding, tabulating and analyzing data. Data was calculated and presented as mean  $\pm$  Standard deviation (SD). Differences in means between diet groups for each parameter were analyzed using independent sample T test. P value that was less than 0.05 was deemed to be significant statistically, and a P value of less than 0.001 was deemed highly statistically significant. All graphic representations of the data were done using Microsoft Excel for windows (Microsoft Inc., USA).

## RESULTS

### [I] Biochemical results:

1) **Insulin resistance (IR):** There was an observed highly significant increase ( $P < 0.001$ ) in insulin resistance level in HFD group when compared with the control group (**Table 1**).

2) **Serum lipid profile:** There was a highly significant increase ( $P < 0.001$ ) in the serum cholesterol, TG and LDL level in the HFD group compared with that of the control group. Additionally, there was a highly significant decrease ( $P < 0.001$ ) in the serum HDL in the HFD group compared with that of the control group (**Fig. 3**).

### [II] Histological results:

1) **Light Microscope using H&E and Periodic acid Schiff /Alcian blue stains:** The sublingual gland sections of the control group showed normal mucous acini consisting of simple columnar cells with flat basal nuclei, pale basophilic spongy cytoplasm and normal connective tissue stroma with a duct system lined by cuboidal cells with central rounded nuclei. On the other hand, HFD sublingual gland sections showed closely packed mucous acinar cells with deeply stained nuclei, irregular intra lobular ducts with some vacuolations, thick, fibrotic connective tissue septa and congested blood vessels (**Fig.1**).

2) **Combined PAS and Alcian blue staining analysis of salivary gland:** The SLG stained sections of the control group showed weak Alcian blue staining, while that of the HFD group showed strong Alcian blue staining (**Fig. 1**).

3) **Alpha smooth muscle actin staining ( $\alpha$  SMA):** Examination of alpha smooth muscle actin immunostained sections revealed positive expression of  $\alpha$  SMA staining in the cytoplasm of

the myoepithelial cells in the peripheral part of the acini in control SLG gland, with increased positive expression in the cytoplasm of the myoepithelial cells in the peripheral part of the acini in HFD group (**Fig. 2**).

4) **Aquaporin 8(AQ8) staining antibodies:** Examination of aquaporin 8 immuno-stained sections revealed a positive expression of AQ8 staining in the cytoplasm of the acinar and ductular cells mainly in the acini and ducts' periphery. AQ8 was also expressed in the cytoplasm of myoepithelial cells surrounding the acini and ducts. On the other hand, the expression of AQ8 was decreased in the HFD group (**Fig. 2**).

### [III] Morphometric results:

At the start of the experiment, there was no significant difference in the body weight and body mass index between the control group and HFD group. After the 3 months' administration of a high fat diet, HFD group showed a highly significant increase in body weight and body mass index when compared with (C) group ( $P < 0.001$ ) & significant increase in the weight of the gland when compared with (C) group ( $P < 0.05$ ) (**Table 1**).

There was a highly significant decrease ( $P < 0.001$ ) in the diameter of acini and ducts of SLG in HFD group compared with that of the control group (**Fig. 4**).

Image analysis using of combined PAS/Alcian blue staining sections showed a highly significant increase ( $P < 0.001$ ) in the optical density of PAS/Alcian blue in HFD group when compared with control group (**Fig. 5**).

Image analysis using alpha smooth muscle actin immunostained sections showed a significant increase ( $P < 0.05$ ) in the area percentage of  $\alpha$  SMA in HFD group with no significant difference ( $P > 0.05$ ) in the optical density of  $\alpha$  SMA positive reaction when compared with control group (**Fig. 4,5**).

By image analysis using of aquaporin 8 immuno-stained sections, there was a highly significant decrease ( $P < 0.001$ ) in the area percentage of AQ8 and significant decrease ( $P < 0.05$ ) in the optical density of AQ8 positive reaction in comparison with the control group (**Fig. 4, 5**).

## DISCUSSION

Previous studies indicated that metabolic syndrome could be induced successfully by the



collective usage of the high-fat and fructose diet models as they have a synergic effect (23). This is shown by the increased deposition of abdominal fat, dyslipidemia, increased systolic blood pressure and impaired glucose tolerance in rats (24), resembling what is called the American Lifestyle-Induced Obesity Syndrome (25). This was evident in this study, as the administration of high fat and fructose diet for 12 weeks resulted in progressive increase in body weight, body mass index, insulin resistance level and hyperlipidemia in comparison with the control group. Hyperlipidemia is marked by increased levels of serum total cholesterol (TC), triglycerides (TG), and low-density lipoprotein (LDL) with a decreased level of high-density lipoprotein (HDL).

The weight of the glands in the high fat diet group was significantly increased in comparison with the control group as observed by previous studies on parotid and submandibular glands, which is a result of enhanced storage of lipid droplets/adipocytes in the gland parenchyma (26, 27).

HFD induced degenerative changes in the form of vacuolated cytoplasm with lipid deposition and congested blood vessels in gland parenchyma. The vacuoles seemed to be made up of lipid as they were removed during the processing and fixation of the samples (28). Congested blood vessels might be a component of an inflammatory response to increase blood flow to the areas of degeneration. (29). The diameter of acini and ducts in HFD rats decreased compared to control gland. The reductions in acinar diameters might suggest glandular atrophy due to acinar cell shrinkage rather as reported in a study done by (30).

The acini of the HFD showed a strong positive alcian blue staining compared to the control group. This can be explained by the degenerative changes in the gland resulting from HFD lead to accumulation of its secretion or changes in the nature of secretion of acid and neutral mucin. There are no studies available describing the effect of HFD on SLG secretion.

Alpha smooth muscle actin is a contractile protein present in the myoepithelial cells around the acini and ducts responsible for squeezing the secretion of the gland (31). HFD SLG glands showed a stronger reaction to  $\alpha$  smooth muscle actin staining than the control group. A similar result to the increased expression of alpha smooth muscle

actin in the HDF group has been previously documented in some studies that showed that morphological and proliferative changes in myoepithelial cells resulted in the increase of their number and size, even when the acini were subjected to atrophy (32) & (33). In stressful conditions, recovery of gland function seemed to require raising the surviving cells' secretory capacity. This needs more MECs to squeeze the accumulated secretion (34).

AQP8 affects the composition of saliva and plays a pivotal role in regulating hydrogen peroxide elimination. In this study, in the HFD model, findings matching published data, with a decreased expression of AQ8 immunostaining was observed in the submandibular gland (16) and in the liver (35) & (36).

Oligonucleotide microarray studies reported that feeding cholesterol to mice down regulates various liver genes including AQP8 (37). Cholesterol down regulated the proteolytic activation of cholesterol-responsive sterol regulatory element binding protein (SREBP) transcriptions factor 1 and 2, and the expression of the target gene 3-hydroxy -3-methylglutaryl-CoA reductase (HMGCR), Under such conditions, mitochondrial aquaporin 8 mRNA and protein expressions were significantly reduced (36). Besides, a recent transomics study suggests mouse liver AQ8 as a cholesterol-related gene (37). The metabolic syndrome is associated with increased reactive oxygen species production (38). H<sub>2</sub>O<sub>2</sub> has contradictory roles; in physiological conditions, it increases signaling of growth factors, but when in excess, causes severe cell damage (39). The peroxiporin AQP8 can be considered as a compensatory protein for H<sub>2</sub>O<sub>2</sub> detoxification. Previous research found that AQP8 knock down  $\beta$ -cells exhibited pronounced sensitivity to reactive oxygen species, resulting in a significant loss of  $\beta$ -cell viability due to enhanced toxicity of the increased concentrations of H<sub>2</sub>O<sub>2</sub> and hydroxyl radicals (\*OH) in mitochondria (40). Noteworthy, oxidative stress conditions inhibit AQP8-mediated H<sub>2</sub>O<sub>2</sub> scavenging, and that, in a vicious circle, contribute to worsening the condition (41). Others showed that the inflammatory cellular infiltration, increased secretion of pro-inflammatory cytokines (TNF $\alpha$ , IL-6, IL-1 $\beta$ ) (42) and increased apoptosis (43) resulting from high fat diet led to gland

degeneration and cellular down regulation of aquaporin 8.

### CONCLUSIONS

In the present study, a decreased AQP8 immunostaining expression was established in the high fat and fructose diet rats which might partially contribute to gland secretory dysfunction.

### ACKNOWLEDGEMENT

This manuscript is part of the master thesis in Anatomy of Amal Saber in the Department of Anatomy, University of Mansoura, Egypt.

### AUTHOR CONTRIBUTIONS

All the authors have accepted responsibility for the entire content of this submitted manuscript and approved its submission.

### ETHICAL APPROVAL

The current study was approved by the Institutional Research Board (IRB) (MS.21.06.1544-2021/07/03), Faculty of Medicine, Mansoura University. It followed the National Institutes of Health (NIH) guidelines for animal care. The study was approved by the local ethical committee on animals' experimentation.

### CONFLICTS OF INTEREST

The authors declared that they have no conflicts of interest with respect to the authorship and/or publication of this article.

### FINANCIAL DISCLOSURES

This study was not supported by any source of funding.

### REFERENCES

- 1- **Bhupathiraju, S. N., & Hu, F. B.** Epidemiology of obesity and diabetes and their cardiovascular complications. *Circ. Res.* 2016; 118(11), 1723-1735.
- 2- **Chauhan, R., & Haslam, D.** Obesity and Periodontal Disease. *Bariatric Surg. Clin. Pract.* 2022; 29-32. Springer, Cham.
- 3- **Weihrauch-Blüher S, Schwarz P, Klusmann JH.** Childhood obesity: increased risk for cardiometabolic disease and cancer in adulthood. *Metab.* 2019 Mar 1; 92:147-152.
- 4- **Lovasi, G. S., Hutson, M. A., Guerra, M., & Neckerman, K. M.** Built environments and obesity in disadvantaged populations. *Epidemiol. Rev.* 2009; 31(1), 7-20.
- 5- **Marques, C., Meireles, M., Norberto, S., Leite, J., Freitas, J., Pestana, D., et al.** High-fat diet-induced obesity Rat model: a comparison between Wistar and Sprague-Dawley Rat. *Adipocyte.* 2016; 5(1), 11-21.
- 6- **Kim, K., Choi, S., Chang, J., Kim, S. M., Kim, S. J., Kim, R. J. Y., et al.** Severity of dental caries and risk of coronary heart disease in middle-aged men and women: A population-based cohort study of Korean adults, 2002–2013. *Sci. Rep.* 2019; 9(1), 1-7.
- 7- **Azad, A. K., Ahmed, J., Hakim, A., Hasan, M., Alum, M., Hasan, M., et al.** Genome-wide characterization deciphers distinct properties of aquaporins in six *Phytophthora* species. *Curr. Bioinform.* 2021;16(6), 880-898.
- 8- **D'Agostino, C., Elk Ashty, O. A., Chivasso, C., Perret, J., Tran, S. D., & Delporte, C.** Insight into salivary gland aquaporins. *Cells.* 2020; 9(6), 1547.
- 9- **Finn, R. N., & Cerda, J.** Evolution and functional diversity of aquaporins. *Biol. Bull.* 2015;229(1), 6-23.
- 10- **Pellavio, G., & Laforenza, U.** Human sperm functioning is related to the aquaporin-mediated water and hydrogen peroxide transport regulation. *Biochimie.* 2021; 188, 45-51.
- 11- **Wellner, R. B., Hoque, A. T. M. S., Goldsmith, C. M., & Baum, B. J.** Evidence that aquaporin-8 is located in the basolateral membrane of rat submandibular gland acinar cells. *Pflug Arch.* 2000; 441 (1), 49-56.
- 12- **Nakamura, M., Saga, T., Watanabe, K., Takahashi, N., Tabira, Y., Kusukawa, J., et al.** An Immunohistochemistry-Based Study on Aquaporin (AQP)-1, 3, 4, 5 and 8 in the Parotid Glands, Submandibular Glands and Sublingual Glands of Sjögren 's Syndrome Mouse Models Chronically Administered Cevimeline. *Kurume Med.J.* 2013; MS60227.
- 13- **13-Loboda A, Damulewicz M, Pyza E, Jozkowicz A and Dulak J.** Role of Nrf2/HO-1 system in development, oxidative stress response and diseases: an evolutionarily conserved mechanism. *Cell Mol Life Sci.* 2016;3: 3221–3247.
- 14- **14-Jensen, V. S., Hvid, H., Damgaard, J., Nygaard, H., Ingvorsen, C., Wulff, E. M., et al.** Dietary fat stimulates development of NAFLD more potently than dietary fructose in Sprague–Dawley rats. *Diabetol. Metab. Syndr.* 2018;10(1), 4.
- 15- **15-Mamikutty, N., Thent, Z. C., Sapri, S. R., Sahruddin, N. N., Mohd Yusof, M. R., & Haji Suhaimi, F.** The establishment of metabolic syndrome model by induction of fructose drinking

water in male Wistar rats. *Biomed Res.Int.* 2014, 263897.

**16- Velasco-Ortega, E., Delgado-Ruiz, R. A., & López-López, J.** Dentistry and diabetes: the influence of diabetes in oral diseases and dental treatments. *J. Diabetes Res.*, 2016, 1.

**17- Warnick, G. R., Knopp, R. H., Fitzpatrick, V., & Branson, L.** Estimating low-density lipoprotein cholesterol by the Friedewald equation is adequate for classifying patients on the basis of nationally recommended cutpoints. *Clin. Chem.*1990;36(1), 15-19.

**18- Ngo HT, Hetland RB, Sabaredzovic A, Haug LS, Steffensen IL.** In utero exposure to perfluorooctanoate (PFOA) or perfluorooctane sulfonate (PFOS) did not increase body weight or intestinal tumorigenesis in multiple intestinal neoplasia (Min/+) mice. *Environ.Res.* 2014 Jul 1; 132:251-263.

**19- Cui, F., Hu, M., Li, R., Li, B., Huang, D., Ma, W., et al.** Insulin on changes in expressions of aquaporin-1, aquaporin-5, and aquaporin-8 in submandibular salivary glands of rats with Streptozotocin-induced diabetes. *Int. J. Clin. Exp. Pathol.*2021; 14(2), 221.

**20- Bhatia, S. K., Rashid, A., Chrenek, M. A., Zhang, Q., Bruce, B. B., Klein, M., et al.** Analysis of RPE morphometry in human eyes. *Mol. Vis.* 2016; 22; 898.

**21- Sisto, M., Lorusso, L., Ingravallo, G., Tamma, R., Nico, B., Ribatti, D., et al.** Reduced myofilament component in primary Sjögren's syndrome salivary gland myoepithelial cells. *J. Mol. histol.*2018;49(2), 111-121.

**22- Almasry, S. M., Habib, E. K., Elmansy, R. A., & Hassan, Z. A.** Hyperglycemia alters the protein levels of prominin-1 and VEGFA in the retina of albino rats. *J. Histochem. Cytochem.*2018; 66(1), 33-45.

**23- Poudyal, H., Panchal, S., & Brown, L.** Comparison of purple carrot juice and  $\beta$ -carotene in a high-carbohydrate, high-fat diet-fed rat model of the metabolic syndrome. *Br. J. Nutr.*2010; 104(9), 1322-1332.

**24- Panchal, S. K., Poudyal, H., Iyer, A., Nazer, R., Alam, A., Diwan, V., et al.** High-carbohydrate, high-fat diet-induced metabolic syndrome and cardiovascular Remodeling in rats. *J. Cardiovasc. Pharmacol.* 2011; 57(5), 611-624.

**25- Tetri, L. H., Basaranoglu, M., Brunt, E. M., Yerian, L. M., & Neuschwander-Tetri, B. A.**

Severe NAFLD with hepatic necro inflammatory changes in mice fed trans fats and a high-fructose corn syrup equivalent *Am.J. Physiol.Gastrointest.* 2008; 295(5), G987-G995.

**26- Kolodziej U, Maciejczyk M, Miąsko A, Matczuk J, Knaś M, Żukowski P, et al.** Oxidative modification in the salivary glands of high fat-diet induced insulin resistant rats. *Front. Physiol.* 2017 Jan 26; 8:20.

**27- de Carvalho PM, Gavião MB, Carpenter GH.** Altered autophagy and sympathetic innervation in salivary glands from high-fat diet mice. *Arch. Oral Biol.* 2017 Mar 1; 75:107-113.

**28- Al-Serwi, R. H., El-Sherbiny, M., Eladl, M. A., Aloyouny, A., & Rahman, I.** Protective effect of nano vitamin D against fatty degeneration in submandibular and sublingual salivary glands: A histological and ultrastructural study. *Heliyon.*2021; 7(4), e06932.

**29- Selim, S. A.** The effect of high-fat diet-induced obesity on the parotid gland of adult male albino rats: histological and immunohistochemical study. *Egypt. J. Histol.* 2013; 36(4), 772- 80.

**30- Scott J. and Gunn DL.** Functional characteristics of atrophic parotid gland acinar cells from rats after liquid feeding. *J. Dent. Res.* 1994; 73, 1180-1186.

**31- Gugliotta PA, Sapino A, Macrí LU, Skalli OM, Gabbiani GI, Bussolati G.** Specific demonstration of myoepithelial cells by anti-alpha smooth muscle actin antibody. *J. Histochem. Cytochem.* 1988 Jun;36(6):659-663.

**32- Buettner R, Scholmerich J, Bollheimer LC.** High fat diets: modeling the metabolic disorders of human obesity in rodents. *Obes.*2007;15:798– 808.

**33- Nunes T, Bernardazzi C, de Souza HS.** Cell death and inflammatory bowel diseases: Apoptosis, necrosis, and autophagy in the intestinal epithelium. *Biomed.Res. Int.* 2014; 1-12.

**34- Al-Refai IAS, Kamal KA, Ali S.** The Effect of Green Tea Extract on Submandibular Salivary Gland of Methotrexate Treated Albino Rats: Immunohistochemical Study Al-Refai et al., *J. Cytol.Histol.*2014; 5(2),1.

**35- Chartoumpakis, D. V., Ziros, P. G., Zaravinos, A., Iskrenova, R. P., Psyrogiannis, A. I., Kyriazopoulou, V. E., et al.** Hepatic gene expression profiling in Nrf2 knockout mice after long-term high-fat diet-induced obesity. *Oxid. Med. Cell. longev.* 2013,1-17.

36- Danielli, M., Capiglioni, A. M., Marrone, J., Calamita, G., & Marinelli, R. A. Cholesterol can modulate mitochondrial aquaporin-8 expression in human hepatic cells. *IUBMB life*.2017; 69(5), 341-346.

37- Williams, E. G., Wu, Y., Jha, P., Dubuis, S., Blattmann, P., Argmann, C. A., et al. Systems proteomics of liver mitochondria function. *Sci*. 2016;352(6291), aad0189.

38- Bhatti, J. S., Bhatti, G. K., & Reddy, P. H. Mitochondrial dysfunction and oxidative stress in metabolic disorders—A step towards mitochondria based therapeutic strategies. *Biochim. Biophys. Acta -Mol. Basis Dis*.2017;1863(5), 1066-1077.

39- Medrano-Fernandez, I., Bestetti, S., Bertolotti, M., Bienert, G. P., Bottino, C., Laforenza, U., et al. Stress regulates aquaporin-8 permeability to impact cell growth and survival. *Antioxid. Redox signal*.2016; 24(18), 1031-1044.

40- Krüger C, Jörns A, Kaynert J, Waldeck-Weiermair M, Michel T, Elsner M, et al. The importance of aquaporin-8 for cytokine-mediated toxicity in rat insulin-producing cells. *FreeRadic.Biol.Med*. 2021 Oct 1; 174:135-143.

41- Pellavio, G., Rui M., Caliozna, L., et al. Regulation of aquaporin functional properties mediated by the antioxidant effects of natural compounds. *Int.J.Mol. Sci*. 2017;18(12). 2665.

42- Halim, M., & Halim, A. The effects of inflammation, aging and oxidative stress on the pathogenesis of diabetes mellitus (type 2 diabetes). *Diabetes Metab. Syndr.: clin. Res. Rev*.2019; 13(2), 1165-1172.

43- Turkmen, K. Inflammation, oxidative stress, apoptosis, and autophagy in diabetes mellitus and diabetic kidney disease: the Four Horsemen of the Apocalypse. *Int. Urol. Nephrol*.2017;49(5), 837-844.

**TABLES**

**Table (1):** The mean value of body weight (gm) and body mass index (BMI) (gm/cm<sup>2</sup>) at the beginning and end of the experiment & weight of the gland & insulin resistance level ± SD of the control and HFD groups.

Groups	Control	HFD
Body wt (gm) at beginning	189 ± 8	189 ± 4.47 #
Body wt (gm) at sacrifices	299.66 ± 8.98	348 ± 5.09**
BMI (gm/cm <sup>2</sup> ) at the beginning	0.189 ± 0.022	0.185 ± 0.016 #
BMI (gm/cm <sup>2</sup> ) at sacrifices	0.195 ± 0.02	0.264 ± 0.03**
Weight of the gland(gm)	0.2 ± 0.017	0.258 ± 0.047*
Insulin resistance	0.06 ± 0.003	0.078 ± 0.004**

\*\*Highly significant difference VS control group (P < 0.001), \*Significant difference VS control group (P < 0.05), #No significant difference VS control group (P > 0.05).



**FIGURES**

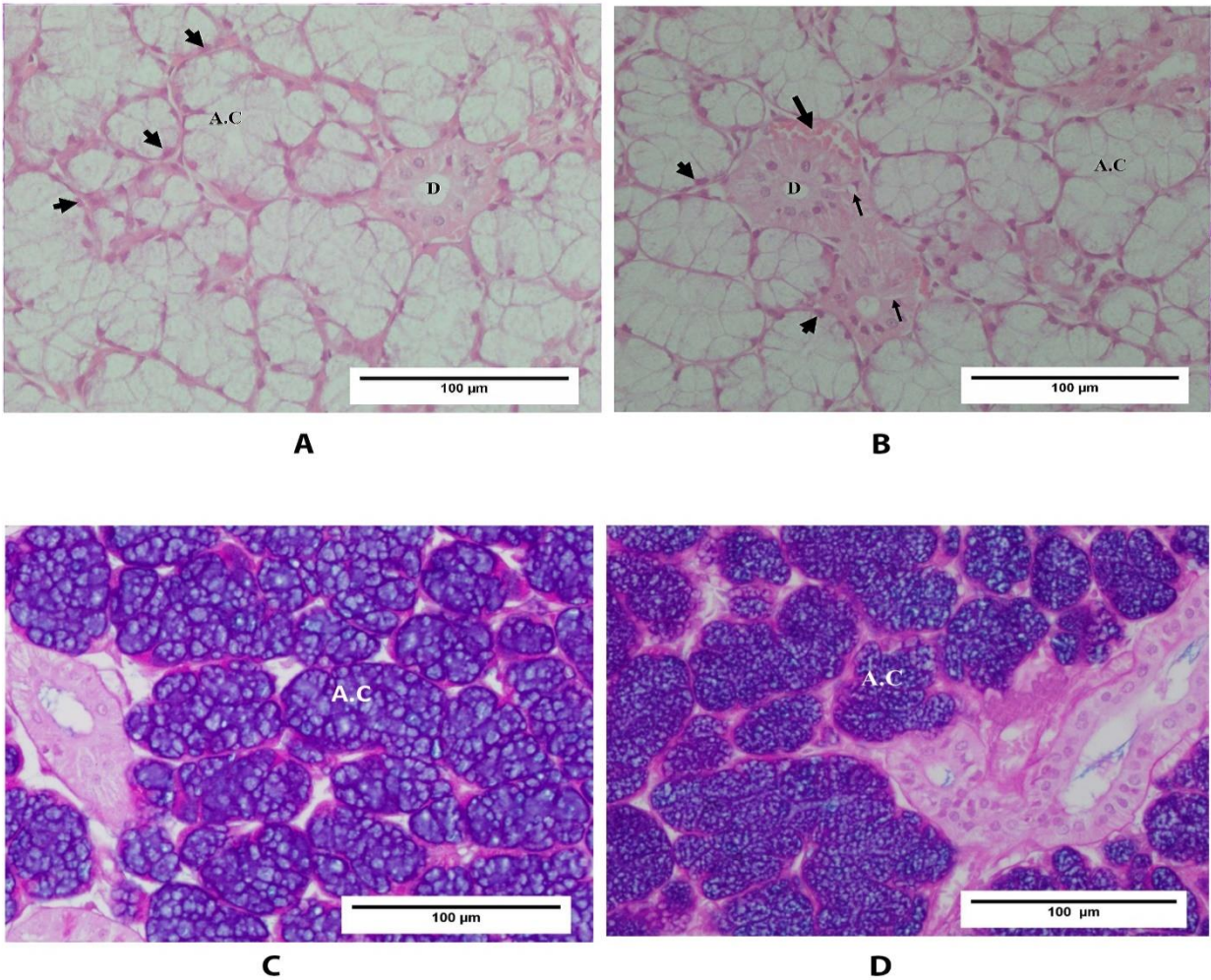


**Figure 1:** Representative photomicrograph of sublingual salivary gland of control and HFD group stained with H&E (1A&1B) respectively and PAS/Alcian blue (1C&1D) respectively. **Fig (1A)** showed mucous acini (A.C) with pale basophilic spongy cytoplasm, flattened basal nuclei (short thick arrow) and interlobular duct (D) lined by cuboidal cells with central rounded nuclei. **Fig (1B)** showed degenerative changes in the form of packed mucous acini (A.C) with densely stained nuclei (short thick arrow), vacuolated cytoplasm (thin arrow), congested blood vessels (long thick arrow) and interlobular duct(D) lined by cuboidal cells with central rounded nuclei. **Fig 1C&1D** showed Positive expression of Alcian blue in the acini (A.C).

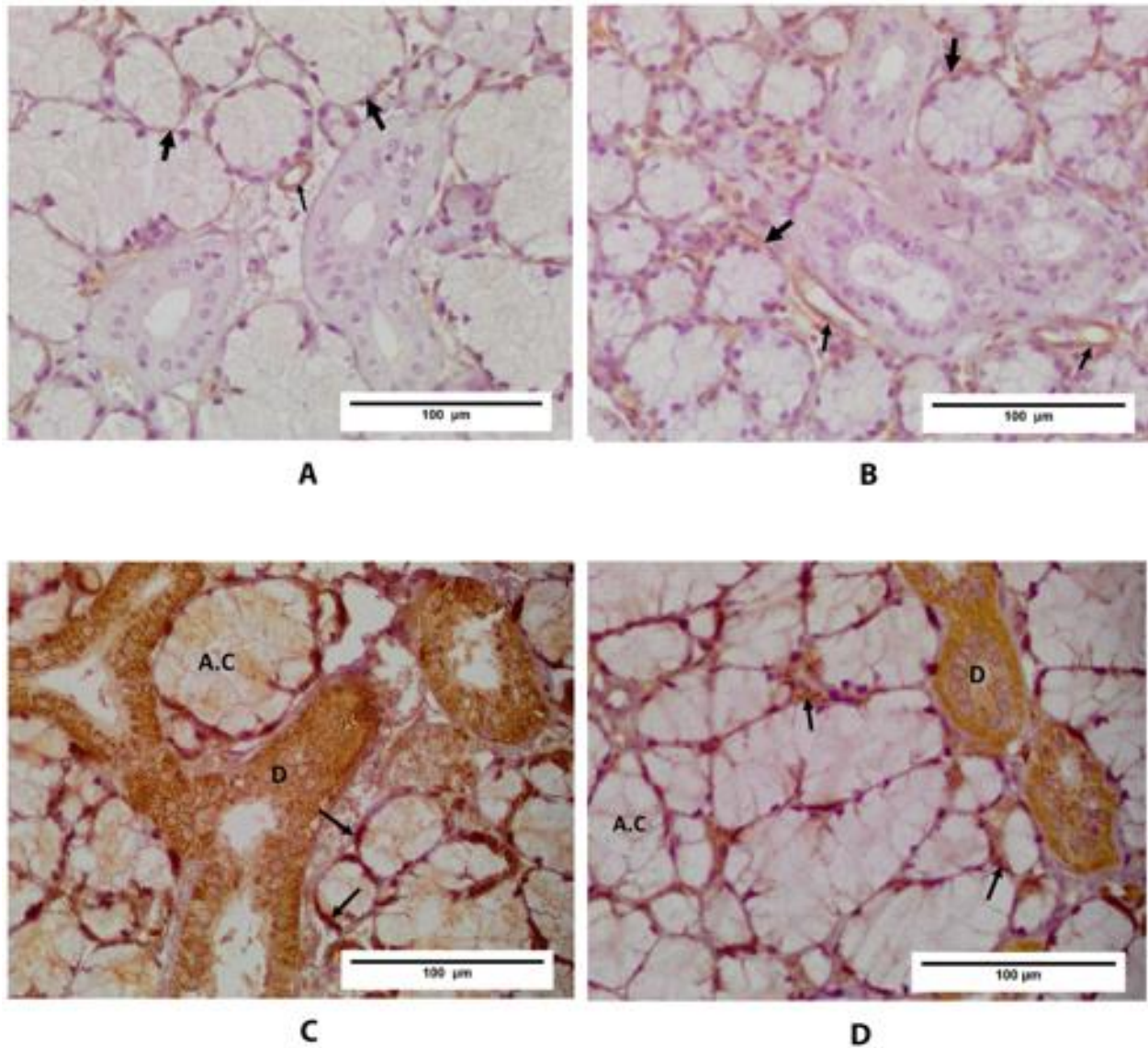


**Figure 2:** Representative photomicrograph of sublingual salivary gland of control and HFD group stained with  $\alpha$  SMA (2A&2B) respectively and AQ8(2C&2D) respectively. Positive cytoplasmic expression  $\alpha$  SMA in the myoepithelial cells around the acini (thick arrow) and endothelial cell (thin arrow) (2A&2B). Positive expression of AQ8 in the cytoplasm of the acini (A.C) & duct (D) and in the myoepithelial cells around acini (thin arrow) (2C&2D).

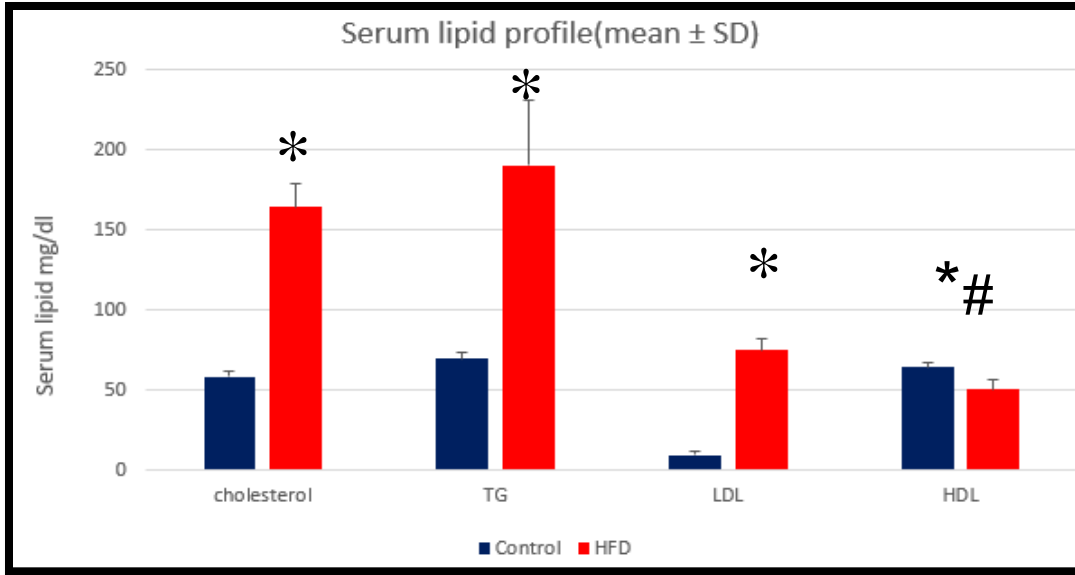


**Figure 3:** Histogram of the mean value of serum lipid profile (mg/dl) ± SD of the two groups.\* Highly significant increase compared to the control group (P<0.001). \* # Highly significant decrease compared to the control group (P<0.001)

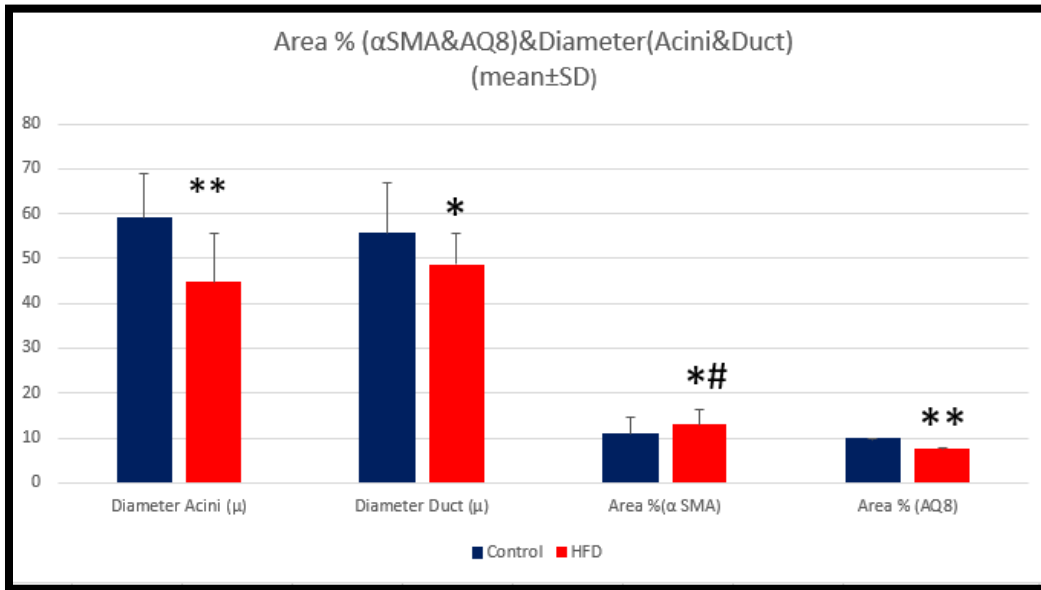


**Figure (4):** Histogram of mean value of the diameter of acini and duct (μ) & area percentage of (AQ8 and α SMA) ± SD of the two groups.\*\* Highly significant decrease compared to the control group (P < 0.001), \* significant decrease compared to the control group (P < 0.05), \*# significant increase compared to the control group (P < 0.05).

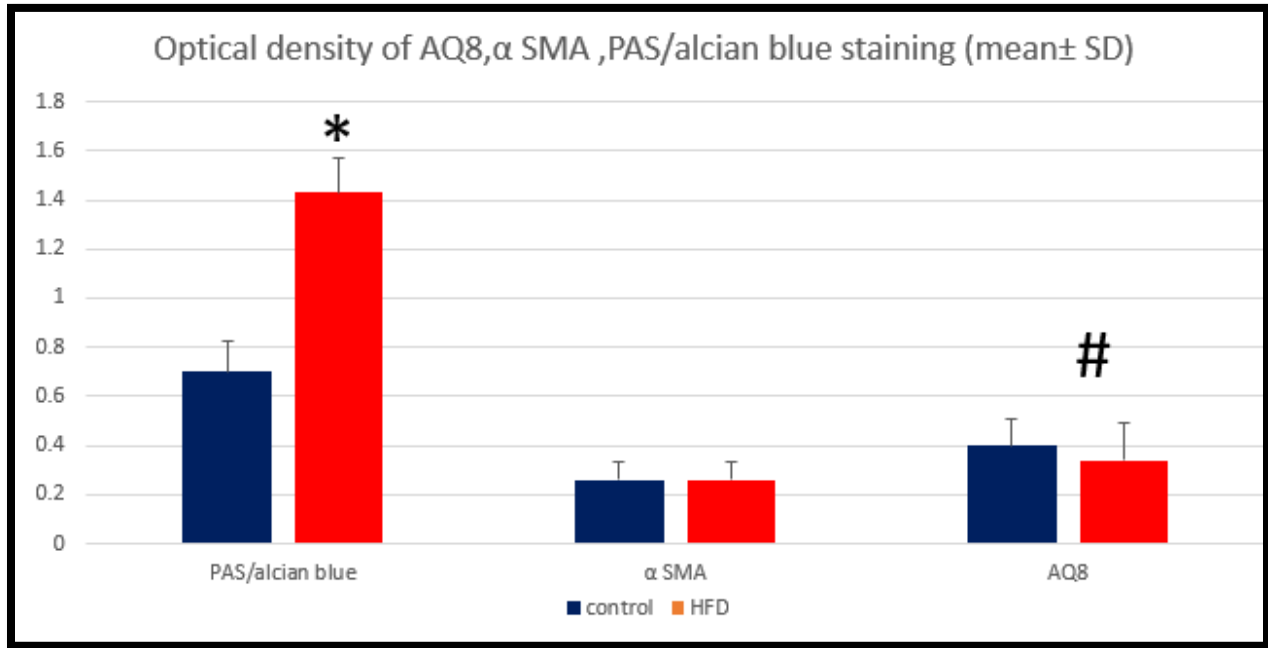


**Figure (5): Histogram of mean value of the optical density of AQ8,  $\alpha$  SMA and PAS/Alcian blue staining  $\pm$  SD of the two groups. \* Highly significant increase compared to the control group. ( $P < 0.001$ ), # Significant decrease compared to the control group. ( $P < 0.05$ ). No significant difference in the optical density of  $\alpha$  SMA of the two groups ( $P > 0.05$ ).**

**To Cite :**

Hamada, A., Hendawy, M., Sherif, R., El Hawary, A. Immunohistochemical Expression of Aquaporin 8 in the Sublingual Salivary gland of High Fat Diet /Fructose Rat Model. *Zagazig University Medical Journal*, 2024; (199-210): -. doi: 10.21608/zumj.2023.182720.2705